

Modern Dyson-Schwinger Equation Studies

M.B. Hecht and C.D. Roberts

*Physics Division, Argonne National Laboratory
Argonne, IL 60439, USA*

(Received: October 26, 2018)

The dichotomy of the pion as QCD's Goldstone mode and a bound state of massive constituents is easily understood using the Dyson-Schwinger equations. That provides the foundation for an efficacious phenomenology, which correlates the pion's charge radius and electromagnetic form factor with its valence quark distribution function; and simultaneously provides a Poincaré covariant description of the nucleon, its form factors and, more recently, meson photoproduction processes. This well-constrained framework can also be used to eliminate candidates for an extension of the Standard Model by providing the relation between current-quark electric dipole moments and that of the neutron.

— A summary of two presentations, one by each author.

1 Introduction

A focus of contemporary studies in QCD is the development of an intuitive understanding of the spectrum and interactions of hadrons in terms of QCD's elementary excitations; i.e., quarks and gluons. Progress can be made by applying a single framework to the calculation of many observables. This facilitates a verification of necessary model assumptions, and the identification of robust correlations between a theory's keystones and hadron properties. Non-hadronic electroweak interactions provide the obvious test bed for any such approach because the electroweak probes are well understood and hence a given experiment yields immediate access to properties of the hadron target. Thus constrained the framework can be used reliably to make predictions for other phenomena, even those far removed from the domain on which it was constrained; e.g., the properties of QCD at nonzero temperature and baryon density.

Herein we supply a brief description of recent progress with the Dyson-Schwinger equations (DSEs) [1] in these applications. A familiar DSE is the gap equation that describes pairing and condensation in low temperature superconductors; another is the Bethe-Salpeter equation, whose solution provides the mass and “wave function” of a bound state in quantum field theory. These are subjects in which the nonperturbative character of DSEs is paramount, to which we will return. However, at their simplest, the DSEs are a generating tool for perturbation theory: the weak coupling expansion of any particular DSE yields all the well-known Feynman diagrams. This is of immense help in studying QCD because it means there is little or no model dependence in the ultraviolet behaviour of calculated quantities. The key model-dependence is limited to the infrared domain, a property that can be exploited to probe the dynamics underlying confinement and dynamical chiral symmetry breaking (DCSB), which are QCD's signature nonperturbative phenomena. The recent successes and current challenges in this application are documented in Refs. [2, 3].

2 Dynamical Chiral Symmetry Breaking

While the dynamical breaking of chiral symmetry in QCD is fundamental to the success of chiral perturbation theory: it is only owing to DCSB that $m_\pi = 0$ in the chiral limit and the scale of f_π is set by the constituent-quark mass, understanding the origin of this phenomenon is outside

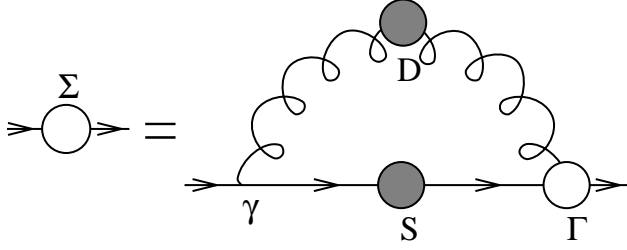


Figure 1: QCD Gap Equation or Dyson-Schwinger equation for the quark self energy, Σ . Here: D is the dressed-gluon propagator; Γ , the dressed-quark-gluon vertex; and $S = 1/[i\gamma \cdot p + m + \Sigma(p)]$, the dressed-quark propagator.

the scope of the theory. This is where QCD's *gap equation*, depicted in Fig. 1, finds immediate application [4]. The solution provides the dressed-quark propagator in terms of the self-energy, Σ :

$$S(p) = 1/[i\gamma \cdot p + m + \Sigma(p)], \quad \Sigma(p) = i\gamma \cdot p[A(p^2) - 1] + B(p^2), \quad (1)$$

where m is the current-quark mass, and the functions $A(p^2)$, $B(p^2)$ are completely determined by the nature of the force between quarks.

Employing a weak coupling expansion yields the perturbative results: $A(p^2) \approx 1$ and

$$B(p^2) = m \left(1 - \frac{3\alpha_s}{4\pi} \ln[p^2/m^2] + \dots \right), \quad (2)$$

where the ellipsis indicates that, like the zeroth and first order contributions, every higher-order term in the perturbative evaluation of $B(p^2)$ is proportional to the current-quark mass. Hence at every finite order in perturbation theory the scalar piece of the quark's self-energy, $B(p^2)$, vanishes in the chiral limit, $m = 0$. Therefore dynamical mass generation, and hence DCSB, is impossible in perturbation theory.

Now the essentially nonperturbative character of DSEs becomes important. The self-energy appears in the denominator of the r.h.s. in Fig. 1 but in the numerator on the l.h.s. This makes the equation nonlinear and hence its self-consistent solution can exhibit properties inaccessible in perturbation theory. Using simple models of the equation's kernel one can unambiguously establish that $B(p^2) \neq 0$ is the favoured solution in the chiral limit if, and only if, the integrand provides sufficient support on the domain $k^2 \in [0, 2] \text{ GeV}^2$; i.e., if the effective coupling in the infrared is *strong enough* [4, 5]. A realistic, one-parameter model of the effective interaction [6] yields the mass function depicted in Fig. 2. It is important to remember that the existence of a nonzero solution in the chiral limit is a purely nonperturbative effect. Hence the domain on which the chiral limit solution and the u -quark solution are nearly indistinguishable is that on which nonperturbative dynamics is dominant in QCD: where they separate marks the beginning of the perturbative domain and this point is characterised by a length-scale of $\sim 0.15 \text{ fm}$.

The quark condensate is a fundamental fitting parameter in chiral perturbation theory. In DSE studies it is a calculated quantity that can simply be read-off from the large- p^2 behaviour of the dressed-quark mass function. In Landau gauge

$$M(p^2) \stackrel{\text{large-}p^2}{\simeq} \frac{2\pi^2\gamma_m}{3} \frac{(-\langle\bar{q}q\rangle^0)}{p^2 \left(\frac{1}{2} \ln \left[\frac{p^2}{\Lambda_{\text{QCD}}^2} \right] \right)^{1-\gamma_m}}, \quad (3)$$

where $\gamma_m = 12/(33 - 2N_f)$, $N_f = 4$, is the anomalous mass dimension, and $\langle\bar{q}q\rangle^0$ is the gauge-invariant and renormalisation-point-independent vacuum quark condensate, which is easily evolved to the mass-scale $\sim 1 \text{ GeV}$ relevant to chiral perturbation theory. The one-parameter model of Ref. [6] yields

$$-\langle\bar{q}q\rangle_{1\text{GeV}}^0 = (0.241 \text{ GeV})^3, \quad (4)$$

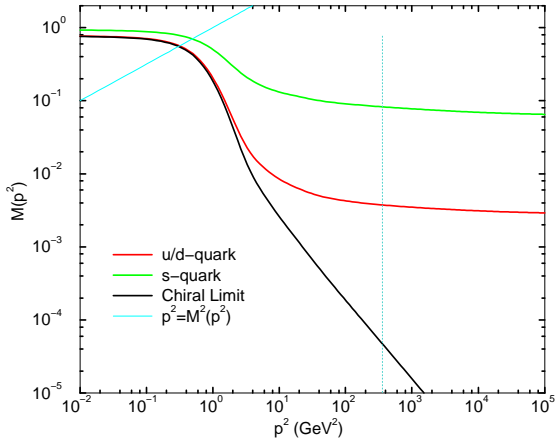


Figure 2: Quark mass function: $M(p^2) = B(p^2)/A(p^2)$, in the chiral limit, and for the u -quark (isospin symmetry is assumed): $m_u^{1\text{GeV}} = 5.5\text{ MeV}$, and the s -quark: $m_s^{1\text{GeV}} = 130\text{ MeV}$. The intersection of the line $p^2 = M^2(p^2)$ with a given curve gives the Euclidean constituent-quark mass [6].

a value consistent with recent lattice simulations [7]. The condensate's value is a QCD analogue of the Cooper pair density in a BCS superconductor, and the value in Eq. (4) corresponds to a density of 1.8 fm^{-3} . Each sphere in a close-packed sea with this density would have a radius $r_{\langle\bar{q}q\rangle} = 0.76\text{ fm}$, which is just 15% larger than the pion's charge radius and 13% less than the proton's. This comparison underscores the importance of a proper description of DCSB in any attempt to explain low-energy phenomena.

3 Mesons

An aim of contemporary experiments is to explore the transition between the nonperturbative and perturbative domains in QCD. That requires momentum transfers at which a theoretical description of the reactions must be Poincaré covariant. For mesons this means employing an homogeneous Bethe-Salpeter equation (BSE) to calculate the mass, and the amplitude that will be used in evaluating necessary matrix elements. (While QCD's gap equation is a DSE for the dressed-quark 2-point function, a propagator, the BSE is a DSE for a 3-point function; i.e., a vertex.) There is a direct connection between the Bethe-Salpeter bound state equation and the vertices that appear in the Ward-Takahashi identities that are a true field theoretical representation of current conservation. The simplest of these identities relate the vertices to the dressed-quark propagator and therefore their fulfillment is only possible if there is a tight connection between the kernel in QCD's gap equation and that in the Bethe-Salpeter equations.

It is a feature of quantum field theory that the Bethe-Salpeter kernel cannot be written in a closed form and hence all concrete calculations must employ a truncation. This is also true of the gap equation's kernel. It is commonplace to find calculations that ignore the constraints applied by the Ward-Takahashi identities, and employ kernels in the the gap equation and the BSE that are incompatible. Such studies necessarily violate the chiral symmetry constraints which the success of chiral perturbation theory has shown to be so important in low-energy QCD. It need not be thus.

3.1 A Mass Formula

There is at least one practical, systematic, symmetry preserving truncation of the DSEs [8]. It has been used [9] to prove Goldstone's theorem in QCD, to obtain quark-level Goldberger-Treiman relations that relate the scalar functions in the pion's Bethe-Salpeter amplitude to those in the dressed-quark propagator, and to derive a mass-formula for flavour nonsinglet pseudoscalar mesons:

$$f_H^2 m_H^2 = -\langle\bar{q}q\rangle_\zeta^H \mathcal{M}_\zeta^H. \quad (5)$$

In this equation: $\mathcal{M}_\zeta^H = m_\zeta^{q_1} + m_\zeta^{q_2}$ is the sum of the current-quark masses of the meson's constituents, with ζ the renormalisation point; the electroweak decay constant is obtained from

$$f_H P_\mu = Z_2(\zeta, \Lambda) \int \frac{d^4 q}{(2\pi)^4} \text{tr} \left[\left(\frac{1}{2} T^H \right)^t \gamma_5 \gamma_\mu \mathcal{S}(q_+) \Gamma^H(q; P) \mathcal{S}(q_-) \right], \quad (6)$$

with $Z_2(\zeta, \Lambda)$ the quark wavefunction renormalisation, Λ the mass-scale in a translationally invariant regularisation of the integral, $q_\pm = q \pm P/2$ (P_μ is the meson's momentum and Γ^H is its bound state amplitude), and, e.g., $T^{\pi^+} = (\lambda^1 + i\lambda^2)/2$, where $\{\lambda^j, j = 1, \dots, 8\}$ are the Gell-Mann matrices, and $(\cdot)^t$ denotes matrix transpose; and the in-hadron condensate is

$$i\langle \bar{q}q \rangle_\zeta^H = f_H Z_4(\zeta, \Lambda) \int \frac{d^4 q}{(2\pi)^4} \text{tr} \left[\left(\frac{1}{2} T^H \right)^t \gamma_5 \mathcal{S}(q_+) \Gamma^H(q; P) \mathcal{S}(q_-) \right]. \quad (7)$$

The Z_2 on the r.h.s. of Eq. (6) ensures that f_H is gauge invariant, and cutoff and renormalisation-point independent; i.e., that it is observable. (Equation (6) is the field theoretical expression for the pseudovector projection of the pion's wavefunction at the origin in configuration space.) Furthermore, the quark-level Goldberger-Treiman relations and Eq. (6) make plain that in the presence of DCSB the magnitude of the pion's leptonic decay constant is set by the constituent-quark mass. The same is true for $\langle \bar{q}q \rangle_\zeta^H$, which, in the chiral limit, is identical to the vacuum quark condensate [9]. The factor Z_4 ensures that the in-hadron condensate is gauge and cutoff independent, and that its renormalisation-point dependence is precisely that required to ensure $\langle \bar{q}q \rangle_\zeta^H \mathcal{M}_\zeta$ is renormalisation-point *in*-dependent.

Equation (5) is written suggestively: it has the appearance of the Gell-Mann–Oakes–Renner relation, and it can be shown [9] that for small current-quark masses it does indeed coincide with that formula. The new aspect of the equation is that it is valid *independent* of the current-quark mass of the constituents: the DSE derivation assumes nothing about the size of $m_\zeta^{q_1, q_2}$. It has consequently been used to prove that the mass of a heavy pseudoscalar meson rises linearly with the mass of its heaviest constituent [10]. Equation (5) is a single mass formula that unifies the light- and heavy-quark domains. It also provides [11] an understanding of recent lattice-QCD data on the current-quark mass-dependence of pseudoscalar meson masses.

The truncation scheme of Ref. [8] is the foundation for a phenomenological model that has been used to very good effect in describing light-quark mesons [6, 12]. That model is the only one to predict [13] a behaviour for the pion's electromagnetic form factor that agrees with the results of a recent Hall C experiment [14]. The large- Q^2 behaviour of the form factor can be obtained algebraically and one finds [15] $Q^2 F_\pi(Q^2) = \text{const.}$, up to logarithmic corrections, in agreement with the perturbative-QCD expectation. This result relies on the presence of pseudovector components in the pion's Bethe-Salpeter amplitude, which is guaranteed by the quark-level Goldberger-Treiman relations proved in Ref. [9].

3.2 Pion's Valence Quark Distribution Function

The DSEs provide a chiral-symmetry preserving, dynamical approach to QCD, which easily captures the dichotomous nature of the pion as: 1) QCD's Goldstone mode; and 2) a bound state of quarks with large constituent-masses, and unifies the low- and high- Q^2 domains. They are therefore well-suited to a study of the pion's valence-quark distribution function, $u_V^\pi(x)$. (This is a measurable expression of the pion's quark-gluon substructure but it cannot be calculated in perturbation theory.) Since π targets are scarce other means must be employed to measure $u_V^\pi(x)$ and one approach is to infer it from πN Drell-Yan [16], which yields $u_V^\pi(x) \propto (1-x)$ for $x \simeq 1$. However, a

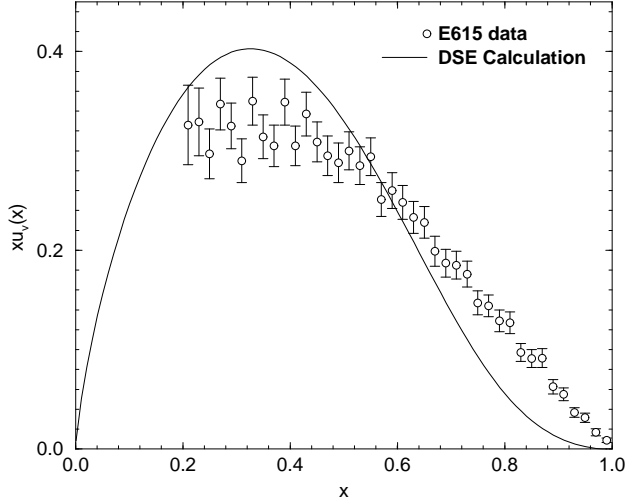


Figure 3: DSE result for $x u_V^\pi(x)$ [17], evolved to $\mu^2 = 16 \text{ GeV}^2$ using the first-order, nonsinglet renormalisation group equation, for direct comparison with the Drell-Yan data [16].

DSE calculation predicts [17]:

$$u_V^\pi(x) \stackrel{x \sim 1}{\propto} (1-x)^2, \quad (8)$$

at a resolving scale of $\mu^2 \simeq 1 \text{ GeV}^2$, and while this conflicts with the extant experimental result, as apparent in Fig. 3, it is consistent with the perturbative-QCD expectation [18]. The discrepancy is very disturbing because a verification of the experimental result would present a profound threat to QCD, even challenging the assumed vector-exchange nature of the interaction. The DSE study [17] has refocused attention on this disagreement, and is the catalyst for a resurgence of interest in $u_V^\pi(x)$ and proposals for its remeasurement [19].

4 Baryons

A direct analogy to treating mesons via the Bethe-Salpeter equation is to describe baryons using a Poincaré covariant Fadde'ev equation. Of course, that equation also involves a kernel about which assumptions must be made in order to arrive at a tractable problem. Here the truncation scheme of Ref. [8] provides, *a posteriori*, a basis for treating baryons as quark-diquark composites using a Fadde'ev equation of the type proposed in Ref. [20]. Therein two quarks are always correlated as a colour-antitriplet diquark quasiparticle (because ladder-like gluon exchange is attractive in the $\bar{3}_c$ quark-quark scattering channel) and binding in the nucleon is effected by the iterated exchange of roles between the dormant and diquark-participant quarks. A first numerical study of this Fadde'ev equation was reported in Ref. [21], and following that there have been numerous more extensive analyses and applications; e.g., Refs. [22, 23], which are reviewed in Ref. [24].

4.1 Fadde'ev Amplitude Ansatz

In developing an efficacious phenomenology it is possible to bypass solving the Fadde'ev equation, which can be a numerically intensive process, and employ a product *Ansatz* for the nucleon's bound state amplitude; an approach kindred to that which is still employed fruitfully in the study of meson properties, e.g., Ref. [25]. The simplest *Ansatz* retains only a scalar (0^+) diquark correlation and models the nucleon's amplitude as [26]:

$$\psi(p_i, \alpha_i, \tau_i) \propto \varepsilon_{c_1 c_2 c_3} [\Gamma^{0^+}(\frac{1}{2}(p_1 - p_2); K)]_{\alpha_1 \alpha_2}^{\tau_1 \tau_2} \Delta^{0^+}(K) [\mathcal{S}(\ell; P)u(P)]_{\alpha_3}^{\tau_3}, \quad (9)$$

	Obs.	Calc.
$(r_p)^2$ (fm ²)	(0.87) ²	(0.78) ²
$(r_n)^2$ (fm ²)	−(0.34) ²	−(0.40) ²
μ_p (μ_N)	2.79	2.85
μ_n (μ_N)	−1.91	−1.61
μ_n/μ_p	−0.68	−0.57
$g_{\pi NN}$	13.4	13.9
$\langle r_{\pi NN}^2 \rangle$ (fm ²)	(0.93-1.06) ²	(0.63) ²
g_A	1.26	0.98
$\langle r_A^2 \rangle$ (fm ²)	(0.68 ± 0.12) ²	(0.83) ²
$g_{\rho NN}$	6.4	5.61
$g_{\omega NN}$	7–10.5	10.0

Table 1: Calculated values of a range of physical observables obtained [26] using the Fadde’ev *Ansatz* parameters in Eq. (12). The ‘‘Obs.’’ column reports experimental values [27] or values employed in a typical meson exchange model [28].

where: (p_i, α_i, τ_i) are the momenta, spin and isospin labels of the quarks comprising the nucleon; $\varepsilon_{c_1 c_2 c_3}$ is the Levi-Civita symbol that gives the colour singlet factor; $P = p_1 + p_2 + p_3$, $K = p_1 + p_2$ and $\ell = (-p_1 - p_2 + 2p_3)/3$; $\Delta^{0^+}(K)$ is a pseudoparticle propagator for the scalar diquark formed from quarks 1 and 2, and Γ^{0^+} is a Bethe-Salpeter-like amplitude describing their relative momentum correlation; \mathcal{S} , a 4×4 Dirac matrix, describes the relative quark-diquark momentum correlation; and $u(P)$ is a free-nucleon spinor. The unknown functions are parametrised as $(\mathcal{F}(x) = (1 - e^{-x})/x)$:

$$\Delta^{0^+}(K) = \frac{1}{m_{0^+}^2} \mathcal{F}(K^2/\omega_{0^+}^2), \quad \Gamma^{0^+}(k; K) = \frac{1}{\mathcal{N}^{0^+}} C i \gamma_5 i \tau_2 \mathcal{F}(k^2/\omega_{0^+}^2), \quad (10)$$

$$\mathcal{S}(\ell; P) = \frac{1}{\mathcal{N}^\psi} \mathcal{F}(\ell^2/\omega_\psi^2) \left[I_D - \frac{R}{M} (i\gamma \cdot \ell - \ell \cdot \hat{P} I_D) \right], \quad (11)$$

where: $C = \gamma_2 \gamma_4$ is the charge conjugation matrix; \mathcal{N}^{0^+} is a calculated normalisation factor that guarantees an electric charge of 1/3 for the scalar diquark; \mathcal{N}^ψ is a similar factor that ensures the proton has unit charge; and $R = 0.5$ measures the ratio of lower to upper component in the nucleon’s spinor in the rest frame, which is taken from Fadde’ev equation studies [11]. The model has three parameters: m_{0^+} , the diquark’s mass; and ω_{0^+} and ω_ψ . They have physical interpretations: $d_{0^+} = 1/m_{0^+}$ is the distance over which a scalar diquark correlation can propagate inside the nucleon; $l_{0^+} = 1/\omega_{0^+}$ is a measure of the mean separation between the quarks in the scalar diquark; and $l_\psi = 1/\omega_\psi$ measures the mean separation between the dormant quark and the diquark.

In the many applications of this *Ansatz* the parameters are typically determined by requiring a least-squares fit to the proton’s electromagnetic form factor, as described in Ref. [26]. The procedure yields (in GeV or fm, as appropriate)

$$\begin{array}{ccc|ccc} m_{0^+} & \omega_{0^+} & \omega_\psi & 1/m_{0^+} & 1/\omega_{0^+} & 1/\omega_\psi \\ \hline 0.62 & 0.79 & 0.23 & 0.32 & 0.25 & 0.86 \end{array} \quad (12)$$

and it is plain that these values provide an internally consistent picture: $l_{0^+} < l_\psi$, which means that the dormant quark is spatially separated from the diquark; and $d_{0^+} < r_p$, the proton’s charge radius, so that the diquark doesn’t propagate outside the nucleon. The subsequent calculated results are then predictions and tests of the model’s fidelity, which can be gauged from Table 1.

4.2 Meson Photoproduction

The same *Ansatz* is being used to study photoproduction of mesons from the nucleon. These processes are important for developing an understanding of the structure of nucleon resonances and in

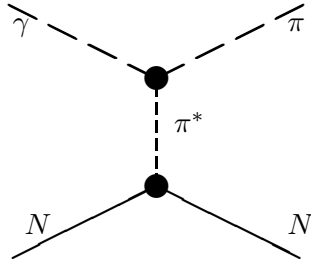


Figure 4: t -channel π -exchange contribution to the π -photoproduction amplitude. In meson exchange models the $\gamma\pi^*\pi$ vertex is usually considered momentum-independent.

searching for “missing” resonances; i.e., those states predicted by constituent quark models that are hitherto unobserved. The aim of these calculations is to provide and constrain the input to meson exchange models, which are the tool that makes possible a comparison with data by subsequently incorporating details of the reaction mechanism. First results for ω photoproduction were presented in Ref. [29] and, while only the t -channel π -exchange mechanism was described, the results at forward angles, where this process must dominate, demonstrate the approach’s promise. A calculation of the contributions to the cross-section from the s - and u -channel processes is almost complete.

Meanwhile the analogous contribution to pion photoproduction, illustrated in Fig. 4, has been calculated and the parameter-free results are depicted in Fig. 5. The solid curve is the Born approximation calculated using an efficacious meson exchange model [31]. That model neglects the necessary momentum dependence of the $\gamma\pi^*\pi$ vertex, for which the DSEs make a prediction. Including the calculated vertex yields the short-dashed curve in Fig. 5, which is not materially different. *A posteriori*, this justifies the meson exchange model expedient of neglecting quark-gluon substructure for these vertices. Of course, with the new DSE predictions, quantitative improvements are now possible. The dashed and dot-dashed curves in Fig. 5 were obtained using the calculated dipole width for the πNN vertex: $F_{\pi NN}(t_\pi)$, which is larger ($\lesssim 2$) than that fitted to data in Ref. [31]. The effect is significant in this case. However, there are preliminary indications that the particularly soft form factor used in the meson exchange model is implicitly also accounting for off-nucleon-mass-shell suppression in the form factor. It is a known property (see, e.g., Ref. [25]) that vertices describing the interaction of three composite objects provide suppression when any one of the attached legs is off-shell. The DSE prediction for the strength of this effect will facilitate the qualitative improvement of meson exchange models by making possible the explicit representation of this phenomenon.

4.3 Neutron’s Electric Dipole Moment

A well-founded description of the nucleon makes many applications possible, even constraining extensions of the Standard Model, which is an important focus of contemporary nuclear and particle physics. It has long been known that the possession of an electric dipole moment (EDM) by a spin-1/2 particle would signal the violation of time-reversal invariance. Any such effect is likely small, given the observed magnitude of CP and T violation in the neutral kaon system, and this makes neutral particles the obvious subject for experiments: the existence of an electric monopole charge would overwhelm most signals of the dipole strength. It is therefore natural to focus on the neutron, which is the simplest spin- $\frac{1}{2}$ neutral system in nature. Attempts to measure the neutron’s EDM, d_n , have a long history and currently [32]

$$|d_n| < 6.3 \times 10^{-26} \text{ e cm (90\% C.L.)}. \quad (13)$$

(NB. $e/(2M_n) = 1.0 \times 10^{-14} \text{ e cm}$. Therefore, writing $d_n = eh_n/(2M)$, where M is the neutron’s mass and h_n is its “gyroelectric ratio,” Eq. (13) corresponds to $|h_n| < 6.0 \times 10^{-12}$.)

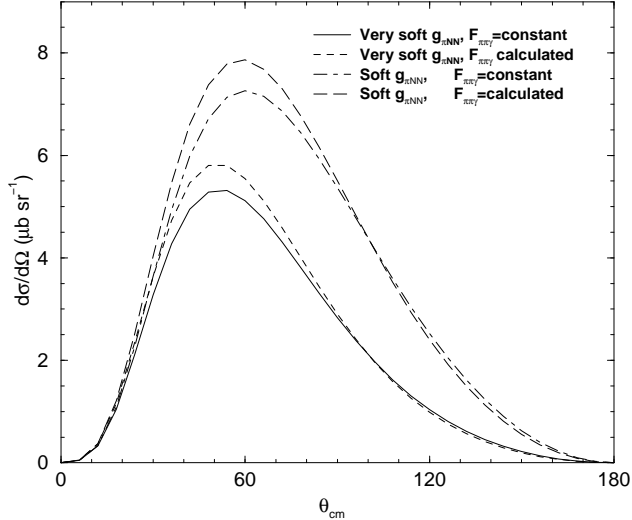


Figure 5: $\gamma N \rightarrow \pi N$ differential cross-section at $E_\gamma = 0.34$ GeV as obtained solely from the Born diagram in Fig. 4. The solid line is the Born cross-section obtained [30] using the meson exchange model of Ref. [31] whose parameters were fitted to data in a full T -matrix calculation. The remaining curves, discussed in the text, are calculated using DSE input.

This experimental constraint on d_n has been very effective in ruling out candidates for theories that enlarge the Standard Model. That is true because in the Standard Model the first nonzero contribution to a free quark’s EDM appears at third order and involves a gluon radiative correction (i.e., $O(\alpha_s G_F^2)$), for the same reason that flavour-changing neutral currents are suppressed: the GIM mechanism) so that [26]

$$d_n^{\text{SM}} \lesssim 10^{-34} e \text{ cm}. \quad (14)$$

This is seven orders-of-magnitude less than the experimental upper bound. However, the Standard Model is peculiar in this regard and candidates for its extension typically contain many more possibilities for CP and T violation, which are not *a priori* constrained to be small. Hence Eq. (13) is an important and direct constraint on these extensions because Eq. (14) indicates that the Standard Model contribution to d_n cannot interfere at a level that could currently cause confusion.

Extensions of the Standard Model are typically used to predict current-quark EDMs, and to proceed from these to a result for d_n one must have an understanding of the relation between current-quarks and constituent-quarks, and a reliable model of the neutron. The DSEs give both: the first from the gap equation, and the second from the Fadde’ev equation studies and their phenomenological application. Putting these elements together one arrives [26] at a quantitative relation between the current-quark’s gyroelectric ratio and that of the neutron: $h_n \approx -91 h_d$. Here the very large magnifying factor: 91, owes its appearance to DCSB, which turns the current-quark into the constituent-quark, and it means that Eq. (13) applies the following bound:

$$|h_d| < 7.4 \times 10^{-14}. \quad (15)$$

(NB. Most extensions of the Standard Model predict $h_u \ll h_d$.) This DCSB-tightened bound very much threatens the viability of a popular three-Higgs-boson model of spontaneous CP violation [33]. Furthermore, and importantly, the result in Eq. (15) is independent of the model used to calculate h_d and hence can be applied directly to constrain any extension of the Standard Model.

5 Epilogue

Owing to dynamical chiral symmetry breaking in QCD the pion appears as both a Goldstone mode and a bound state of massive constituents. The existence of at least one systematic, symmetry preserving truncation scheme makes a detailed understanding and explanation of this phenomenon

possible using the Dyson-Schwinger equations (DSEs). This is the starting point for a successful phenomenology of strong interaction phenomena, which quantitatively and qualitatively unifies the low- and high-energy regimes. Since the DSEs maintain contact with perturbation theory, the model-dependence is restricted to a statement about the infrared behaviour of the quark-quark interaction; i.e., the unknown nature of the long-range force in QCD. This remaining model-dependence is a virtue because it makes possible the correlation of observables via a parametrisation of this infrared behaviour and hence the use of experiments as a probe of the confining force.

Acknowledgments: This work was supported by the US Department of Energy, Nuclear Physics Division, under contract no. W-31-109-ENG-38.

References

- [1] C.D. Roberts and A.G. Williams, *Prog. Part. Nucl. Phys.* **33**, 477 (1994).
- [2] C.D. Roberts and S.M. Schmidt, *Prog. Part. Nucl. Phys.* **45**, S1 (2000).
- [3] R. Alkofer and L. v. Smekal, *Phys. Rept.* **353**, 281 (2001).
- [4] For a pedagogical introduction see: C.D. Roberts, “Nonperturbative QCD with Modern Tools,” in *Frontiers in Nuclear Physics*, edited by S. Kuyucak (World Scientific, Singapore, 1999) pp. 212-261.
- [5] C.D. Roberts, “Continuum strong QCD: Confinement and dynamical chiral symmetry breaking,” *nucl-th/0007054*.
- [6] P. Maris and C.D. Roberts, *Phys. Rev. C* **56**, 3369 (1997).
- [7] P.C. Tandy, “Soft QCD modeling of meson electromagnetic form factors,” *nucl-th/0106031*.
- [8] A. Bender, C.D. Roberts and L. v. Smekal, *Phys. Lett. B* **380**, 7 (1996).
- [9] P. Maris, C.D. Roberts and P.C. Tandy, *Phys. Lett. B* **420**, 267 (1998).
- [10] M.A. Ivanov, Yu.L. Kalinovskiy and C.D. Roberts, *Phys. Rev. D* **60**, 034018 (1999).
- [11] M.B. Hecht, C.D. Roberts and S.M. Schmidt, “Contemporary applications of Dyson-Schwinger equations,” *nucl-th/0010024*.
- [12] P. Maris, these proceedings.
- [13] P. Maris and P.C. Tandy, *Phys. Rev. C* **61**, 045202 (2000).
- [14] J. Volmer *et al.* [The Jefferson Lab F_π Collaboration], *Phys. Rev. Lett.* **86**, 1713 (2001).
- [15] P. Maris and C.D. Roberts, *Phys. Rev. C* **58**, 3659 (1998).
- [16] J.S. Conway *et al.*, *Phys. Rev. D* **39**, 92 (1989).
- [17] M.B. Hecht, C.D. Roberts and S.M. Schmidt, *Phys. Rev. C* **63**, 025213 (2001).
- [18] S.J. Brodsky, M. Burkardt and I. Schmidt, *Nucl. Phys. B* **441**, 197 (1995).
- [19] R.J. Holt and P.E. Reimer, “Structure of the Goldstone bosons,” *nucl-ex/0010004*; K. Wijesooriya, *et al.*, “The $H(e, e'n)X$ Reaction and the Pion Structure Function,” proposal no. JLab PR01-110.
- [20] R.T. Cahill, C.D. Roberts and J. Praschifka, *Austral. J. Phys.* **42**, 129 (1989).
- [21] C.J. Burden, R.T. Cahill and J. Praschifka, *Austral. J. Phys.* **42**, 147 (1989).
- [22] H. Asami, N. Ishii, W. Bentz and K. Yazaki, *Phys. Rev. C* **51**, 3388 (1995); H. Mineo, W. Bentz and K. Yazaki, *ibid.* **60**, 065201 (1999).
- [23] M. Oettel, M.A. Pichowsky and L. von Smekal, *Eur. Phys. J. A* **8**, 251 (2000); M. Oettel, R. Alkofer and L. von Smekal, *Eur. Phys. J. A* **8**, 553 (2000).
- [24] M.A. Pichowsky, these proceedings.
- [25] M.A. Pichowsky, S. Walawalkar and S. Capstick, *Phys. Rev. D* **60**, 054030 (1999).
- [26] M.B. Hecht, C.D. Roberts and S.M. Schmidt, *Phys. Rev. C* **64**, 025204 (2001).
- [27] K.L. Miller *et al.*, *Phys. Rev. D* **26**, 537 (1982); T. Kitagaki *et al.*, *Phys. Rev. D* **28**, 436 (1983); S. Kopecky, P. Riehs, J.A. Harvey and N.W. Hill, *Phys. Rev. Lett.* **74**, 2427 (1995); S.G. Karshenboim, *Can. J. Phys.* **77**, 241 (1999); D.E. Groom *et al.*, *Eur. Phys. J. C* **15**, 1 (2000).
- [28] T. Sato and T.S. Lee, *Phys. Rev. C* **54**, 2660 (1996).

- [29] M.B. Hecht, C.D. Roberts and S.M. Schmidt, “The character of Goldstone bosons,” nucl-th/0106011.
- [30] T.-S.H. Lee, private communication.
- [31] T. Sato and T.-S.H. Lee, Phys. Rev. C **54**, 2660 (1996).
- [32] P.G. Harris, *et al.*, Phys. Rev. Lett. **82**, 904 (1999).
- [33] S. Weinberg, Phys. Rev. Lett. **37**, 657 (1976).